NIH Public Access
Author Manuscript
Transl Neurosci. Author manuscript; available in PMC 2011 September 22.

Published in final edited form as:
Transl Neurosci. 2011 March ; 2(1): 13–22. doi:10.2478/s13380-011-0002-9.

VOLTAGE-GATED CALCIUM CHANNELS ARE NOT AFFECTED BY THE NOVEL ANTI-EPILEPTIC DRUG LACOSAMIDE

Yuying Wang[1,2] and **Rajesh Khanna**[1,2,*]

[1]Department of Pharmacology and Toxicology, Indiana University, School of Medicine, Indianapolis, IN 46202, USA

[2]Paul and Carole Stark Neurosciences, Research Institute, Indiana University, School of Medicine, Indianapolis, IN 46202, USA

Abstract

The novel anti-epileptic drug lacosamide targets two proteins – voltage-gated sodium channels and collapsin response mediator protein 2 (CRMP-2) – suggesting dual modes of action for lacosamide. We recently identified the neurite outgrowth and axonal guidance protein CRMP-2 as a novel partner and regulator of the presynaptic N-type voltage-gated Ca^{2+} channel (CaV2.2) [Brittain *et al., J. Biol. Chem*. 284: 31375–31390 (2009)]. Here we examined the effects of lacosamide on voltage-gated Ba^{2+} channels. Lacosamide did not affect Ba^{2+} currents *via* N- and P/Q- channels in rat hippocampal neurons or L-type Ca^{2+} channels in a mouse CNS neuronal cell line, respectively. N-type Ba^{2+} currents, augmented by CRMP-2 expression, were also unaffected by acute or chronic lacosamide exposure. These results establish that the anti-epileptic mode of action of lacosamide does not involve these voltage-gated Ca^{2+} channels.

Keywords

CaV2.2/N-type Ca^{2+} channels; Hippocampal neurons; CAD cells; L-type Ca^{2+} channels; Lacosamide

1. Introduction

Epilepsy is a serious medical condition characterized by seizures that result from spontaneous disturbances of the brain's normal electrical activity [1]. To combat two hallmarks of seizure generation – hyperexcitability of neurons and hypersynchrony of neural circuits – an arsenal of antiepileptic drugs (AEDs) have been developed. These AEDs act by potentiating inhibitory pathways within the central nervous system, inhibiting excitatory glutamatergic pathways, or inhibiting excessive neuronal firing [2]. Approximately 20–30% of people with epilepsy continue to have seizures despite the use of existing AEDs and an even larger percentage suffers from treatment side-effects of AEDs. Thus, there is an urgent need for more effective and better-tolerated drug treatments. Lacosamide (LCM, Vimpat®) is a new anticonvulsive drug in use as adjunctive therapy for partial-onset seizures and diabetic neuropathic pain [3,4].

Preclinical studies have identified two targets of LCM's actions. Lacosamide exerts a unique action on its presumed pharmacotherapeutic target, the voltage-gated sodium channels

© Versita Sp. z o.o.

*khanna5@iupui.edu.

NIH-PA Author Manuscript
NIH-PA Author Manuscript
NIH-PA Author Manuscript

NIH-PA Author Manuscript

NIH-PA Author Manuscript

NIH-PA Author Manuscript

(VGSCs), by selectively enhancing the transition to a slow-inactivated state of the channel [3,5,6]. This ability to preferentially block the electrical activity of neurons that are chronically depolarized compared with those at more normal resting potentials sets LCM apart from classical VGSC-targeted AEDs such as carbamazepine, phenytoin, and lamotrigine [6]. Lacosamide's second target, as identified in proteomic and radioligand binding studies [3], is the collapsin response mediator protein 2 (CRMP-2). Using a combined chemical and proteomics approach, Kohn and colleagues showed enantioselective LCM labeling of expressed as well as endogenous brain CRMP-2 [7]. Neither of these reports, however, addressed the mechanism of this interaction, nor did it address any additional pathways that could be affected by LCM's interaction with CRMPs.

CRMPs (also known as *UNC-33*-like proteins (Ulip), dyhropyriminidase-related protein (DRP), TOAD (turned on after division) and TUC (TOAD/Ulip/DRP)), are a family of five intracellular phosphoproteins implicated in neurite outgrowth and axonal guidance [8–10]. While highest during development, in the adult, CRMPs are expressed in brain regions capable of axonal outgrowth, neurogenesis, and synaptic rearrangements [10]. Such rearrangements of synaptic connectivity and aberrant neuronal growth have been observed in epilepsy [11]. At least two studies have reported altered CRMP-2 levels in epilepsy. The first showed a decrease in CRMP-2 levels in brains from patients with mesial temporal lobe epilepsy that was refractory to treatment [12]. The second reported decreased CRMP-2 levels in thalamuses of mice with absence seizures [13]. However, the mechanism by which CRMPs contribute to the pathophysiology of epilepsy is unclear. We hypothesize that LCM, by binding to CRMP-2, may prevent the aberrant synaptic connectivity and/or rearrangements seen in epilepsy. Lacosamide's interaction with CRMP-2 associated proteins can influence the development/progression of epilepsy.

We recently identified a direct interaction between CRMP-2 and N-type voltage-gated Ca^{2+} channels (CaV2.2) that led to increased Ca^{2+} current density via increased surface CaV2.2 expression which, together with CRMP-2-mediated increase in synaptic vesicle recycling, translated into an increased neurotransmitter release [14]. These results positioned CRMP-2 as a novel modulator of presynaptic release. While the roles of Ca^{2+} in transmitter release [15–18] and Ca^{2+} dysregulation in epilepsy [19,20] have been unequivocally demonstrated, it is not known if LCM can modulate Ca^{2+} channels via its action on CRMPs to prevent seizure activity. Therefore, in this study, we tested the effects of LCM on voltage-gated Ca^{2+} channels in cells with (1) endogenous and (2) over-expressed levels of CRMP-2. Our results provide definitive evidence that the full mode of action of the anti-epileptic effect of lacosamide does not involve voltage-gated Ca^{2+} channels.

2. Methods

2.1 Primary Hippocampal Neuronal Cultures

Procedures involving animals and their care were in accordance with the Guide for the Care and Use of Laboratory Animals (National Institutes of Health publication 85–23, Bethesda, MD, USA) and approved by the Institutional Animal Care and Use Committee of the Indiana University School of Medicine (Approval # 3181). Pregnant Sprague-Dawley rats were purchased from Harlan Laboratories (Indianapolis, IN). Rat hippocampal neuron cultures were prepared from hippocampi dissected from postnatal day 1 (PN1) rats as described previously [21–23]. Briefly, rat hippocampi were dissected out of PN1 rats, and cells were dissociated enzymatically and mechanically (trituration through Pasteur pipette) in a Papain solution (12 U/ml; Worthington, Freehold, NJ) containing Leibovitz's L-15 medium (Invitrogen), 0.42 mg/ml cysteine (Sigma), 250U/ml DNase 1 (type IV; Sigma), 25 mM $NaHCO_3$, penicillin (50 U/ml)/streptomycin (50 μg/ml), 1 mM sodium pyruvate, and 1 mg/ml glucose (Invitrogen). After dissociation, the cells were gently washed by sequential

NIH-PA Author Manuscript

NIH-PA Author Manuscript

NIH-PA Author Manuscript

centrifugation in Neurobasal medium containing either 2 mg/ml or 20 mg/ml BSA and Pen/Strep, glucose, pyruvate, and DNase1 (as above) and then plated on poly-D-lysine-coated Aclar coverslips at high density (~2000 cells/mm^2). Growth media (1 ml/well) consisted of Neurobasal medium containing 2% NuSerum, 2% B27 (or 5% NS21 [24]), supplemented with penicillin/streptomycin (100 U/ml; 50 μg/ml), 0.1 mM L-Glutamine and 0.4 mM L-glutamax (Invitrogen). Cytosine β-D-arabinofuranoside (5 μM; Sigma) was added 48 h after plating to reduce the number of non-neuronal cells. After 4 d in culture and 2′ each week thereon, half of the growth medium was replaced with medium without cytosine β-D-arabinofuranoside.

2.2 Catecholamine A differentiated (CAD) cells

CAD cells were grown at 37°C and in 5% CO_2 (Sarstedt, Newton, NC) in Ham's F12/EMEM medium (GIBCO, Grand Island, NY), supplemented with 8% fetal bovine serum (FBS; Sigma, St. Louis, MO) and 1% penicillin/streptomycin (100% stocks, 10,000U/ml penicillin G sodium and 10,000 μg/ml streptomycin sulfate). Cells were passaged every 6–7 days at a 1:25 dilution as described [25].

2.3 Transfection

Adherent hippocampal cultures or CAD cells were transfected with cDNAs using Lipofectamine 2000 (Invitrogen) as per the manufacturer's instructions. We routinely achieved about 5% transfection efficiencies in hippocampal neurons transfected with this method. Typically, cultured neurons were transfected with equal amounts of different cDNA constructs at 7–10 days *in vitro* (DIV), and electrophysiology experiments performed two days later.

2.4 Whole-Cell Patch-Clamp Recordings

Whole-cell voltage recordings were performed at room temperature on primary cultured hippocampal neurons or CAD cells using an EPC 10 Amplifier (HEKA Electronics, Germany). Electrodes were pulled from thin-walled borosilicate glass capillaries (Warner Instruments, Hamden, CT) with a P-97 electrode puller (Sutter Instrument, Novato, CA) such that final electrode resistances were 2–3 MΩ when filled with internal solutions. The compositions of the internal and external recording solutions are listed in Table 1. Ba^{2+} was used as the charge carrier as (i) it exhibits greater permeability through voltage-gated Ca^{2+} channels resulting in larger current amplitudes (this is advantageous in neurons from neonatal animals which typically have small currents); (ii) does not elicit as much Ca^{2+}-dependent Ca^{2+} channel inactivation as Ca^{2+}; and (iii) blocks K^+ channels. Ba^{2+} has been reported to shift the current-voltage curve towards more hyperpolarized potentials [26].

Whole-cell capacitance and series resistance were compensated with the amplifier. Series resistances compensation (70–80%) was routinely applied. Cells were considered only when the seal resistance was more than 1 GΩ and the series resistance was less than 10 MΩ. Linear leak currents were digitally subtracted by P/4.

2.5 Data Acquisition and Analysis

Signals were filtered at 10 kHz and digitized at 10–20 kHz. Analysis was performed using Fitmaster and origin8.1 (OriginLab Corporation, MA, USA). For activation curves, conductance (G) through ion (Na^+ and Ca^{2+}) channels was calculated using the equation $G = I/(V_m - V_{rev})$, where V_{rev} is the reversal potential, V_m is the membrane potential at which the current was recorded, and I is the peak current. Activation and inactivation curves were fitted to a Boltzmann function $G/G_{max} = 1/\{1+\exp[(V-V_m)/k]\}$, where G is the peak conductance, G_{max} is the fitted maximal G, V_{50} is the half-activation voltage, and k is the

NIH-PA Author Manuscript

NIH-PA Author Manuscript

NIH-PA Author Manuscript

slope factor. Activation time constant (t) for Ca^{2+} channels was measured by Fitmaster at each command voltage from −40 mV to +30 mV. Additional details of specific pulse protocols are described in the results text or figure legends. For clarity of presentation CAD cell Ba^{2+} currents (see Figure 3A) were filtered with a Savitzky-Golay smoothing method with second order polynomial regression (Origin 8.0 software) while preserving peak current and biophysical properties.

2.6 Chemicals and Solutions

All reagents were purchased from Sigma (St. Louis, MO) unless otherwise indicated. Lacosamide (*R*-2-acetamido-*N*-benzyl-3-methoxypropionamide) was purchased from Cayman Chemicals (Ann Arbor, MI). A 100 mM solution was made up in N-Methylpyrrolidone (MPL) and stored in small aliquots at −20°C. Lidocaine hydrochloride was purchased from Sigma-Aldrich (St. Louis, MO). The final concentration of MPL in physiological solutions was less than 0.3% (v/v). Lacosamide was applied onto the cells through a custom made Y-tube micro-perfusion system. A concentration of 300 μM was used because this represents about 3 times the value at which LCM shows anti-convulsant effects in *in vitro* studies [27] and approximately 5-fold the reported value for half-maximal inhibition of spontaneous excitatory postsynaptic currents and inhibitory postsynaptic currents [28]. The N-type calcium channel blocker omega-conotoxin GVIA (ω-CTX) and the P/Q-type calcium channel blocker omega-agatoxin IVA (ω-Aga) were purchased from Alomone Labs (Jerusalem, Israel).

3. Results

3.1 Lacosamide does not affect N- or P/Q-type voltage-gated Ca^{2+} currents in primary hippocampal neurons

There is only one previous report on the effects of LCM on voltage-gated Ca^{2+} currents which found no effects on Ca^{2+} channel inhibition following acute administration of 100 μM LCM in cortical neurons [28]. No biophysical characterization of the Ca^{2+} currents or chronic administrations of LCM were tested in this study. We recently reported a novel interaction between N-type voltage-gated Ca^{2+} channels and CRMP-2 which lead to an increase in Ca^{2+} currents in hippocampal neurons [14] and dorsal root ganglion sensory neurons [29]. To test if LCM (at 300 μM) can affect properties of N-type voltage-gated Ca^{2+} currents via CaV2.2, we measured whole-cell Ba^{2+} currents in cultured hippocampal neurons. At 10 DIV, N-type Ca^{2+} channels account for ~50% of the total high-voltage activated Ba^{2+} current with P/Q-type channels supporting ~25% [14,30] and R-type supporting less than 3% [26]. Current-voltage (*I*–*V*) relationships were examined by the application of 200-ms voltage steps to various test potentials from a holding potential of −80 mV. Peak inward Ba^{2+} currents were measured and expressed as peak current density (pA/pF) to account for variations in cell size. A representative family of current traces is shown in Figure 1A. Untreated neurons showed a peak density of −16.1 ± 2.2 pA/pF (n=9), which was not different from peak density obtained in neurons treated with 300 μM LCM for 30 min (−16.5 ± 1.0 pA/pF (n=4), 3h (−15.9 ± 2.2 pA/pF (n=9)) and 24 h (−15.0 ± 2.1 pA/pF (n=10)) ($p>0.05$; Student's t-test; Figure 1B, C). A majority amount (~60%) of the Ba^{2+} current in these neurons was conducted via CaV2.2 as assessed from the block observed upon perfusion of the N-type selective blocker ω-conotoxin GVIA (1 mM), while ~85–90% could be blocked by concomitant application of w-conotoxin GVIA and the P/Q-type blocker ω-Agatoxin IVA (500 nM: Figure 1C). We did not directly examine the role of either R- or T-type Ca^{2+} channels which have been reported to be expressed in hippocampal neurons at this stage of culture [31,32]. The relatively minor contribution (<3%) of R-type currents to the total Ca^{2+} current combined with the apparent lack of selectivity of the presumed R-type selective blocker, the spider toxin SNX-482 [33], precluded assessment of

NIH-PA Author Manuscript

NIH-PA Author Manuscript

NIH-PA Author Manuscript

R-type currents in these experiments. Additionally, under our recording conditions, we did not observe any detectable levels of T-types currents (n>50 cells). This conclusion is based on the following observations from our recordings. First, the currents do not inactivate as rapidly or as much (Figure 1A) as has been reported for T-type currents [31,32]. Second, no appreciable current is present at −30 mV, a voltage at which T-type currents have reached their peak [31,32,34]. Third, less than 20% of neurons express 2–3 pA/pF of T-type current [35], which is at most one-fifteenth of the total peak N- and P/Q-type (i.e. non-L-type) current observed in our experiments and within the noise to be confidently assessed as T-type. Moreover, in a published review of LCM's preclinical properties, it was reported that 100 mM does not affect low-voltage activated T-type calcium channels in cortical neurons [28]. As Nifedipine has been reported to partially block T-type currents [26], we cannot completely rule out the possibility that a small fraction of currents in our recordings could be due to T-type. However, as there was no difference in current densities of LCM-treated neurons in the presence or absence of Nifedipine, a contribution of T-type currents, if any, is likely to be negligible.

We also tested the effects of LCM on steady-state activation and inactivation of Ba^{2+} channel gating (Figure 1D, E). The steady-state activation of Ba^{2+} channels in control and LCM-treated neurons was described by the Boltzmann relation. As shown in Table 2, LCM treatment (300 μM) for up to 3 days did not change the gating properties of Ba^{2+} currents as none of the midpoints of activation, inactivation or slopes were affected by LCM treatment.

3.2 Lacosamide does not affect N- or P/Q-type voltage-gated currents in CRMP-2 overexpressing hippocampal neurons

Having established that Ca^{2+} currents are not affected by acute and chronic administration of LCM, we next examined if LCM affected Ca^{2+} currents in CRMP-2 overexpressing hippocampal neurons. CRMP-2 over-expression leads to an ~60% increase in peak Ca^{2+} current density in hippocampal neurons [22]. Consistent with these previous findings, we observed a significant increase of ~58% in Ba^{2+} current in CRMP-2-overexpressing neurons compared to untransfected neurons: CRMP-2 overexpressing neurons had a peak density of −26.7 ± 1.4 pA/pF (n=12) compared to −16.9 ± 3.2 pA/pF (n=7) in untreated neurons (compare Figure 2A, B to Figure 1B, C). Treatment with 300 μM LCM for 3 h did not affect the current-voltage relationship or the peak current density (−26.4 ± 2.3 (n=12)) in CRMP-2 overexpressing neurons (Figure 2A, B). Steady-state activation parameters also were not different between the two groups (Control: V_{50} −25.2 ± 1.9 mV, *k* 11.6 ± 1.8, n=3; 300 μM LCM: V_{50} −32.2 ± 1.8 mV; *k*, 13.2 ± 2.0, n=4; $p > 0.05$; Student's t-test; Figure 2C, D). Activation time constants, measured from single exponential fits to the activation phase of the inward current, were not different between −40 mV and +30 mV between the two groups of neurons ($p > 0.05$, Student's t-test; Figure 2E). Peak tetrodotoxin-sensitive Na^{+} currents from these neurons were blocked by ~65±9% (n=4) following bath application of LCM (Figure 2F), ruling out the possibility that the lack of observed effects on Ba^{2+} currents were from inactive LCM. Collectively, these results suggest that acute and chronic treatment with LCM does not affect Ba^{2+} currents irrespective of the levels of CRMP-2.

3.3 Lacosamide does not affect L-type voltage-gated Ca^{2+} currents in CRMP-2 overexpressing CAD cells

We also examined if LCM affected L-type voltage-gated Ca^{2+} currents in a catecholaminergic cell line (CAD) [36]. CAD cells were chosen for these studies as they are easily amenable to genetic manipulation, are of neuronal origin, and express only L-type Ca^{2+} channels [36]. Inward Ba^{2+} currents that typically inactivated almost completely were observed in these cells (Figure 3A). As reported earlier [36], the threshold for activation of these currents was around −50 mV and the maximum value occurred between −20 to −10

NIH-PA Author Manuscript

NIH-PA Author Manuscript

NIH-PA Author Manuscript

mV (Figure 3B). The inward currents were blocked by >95% with the dihydropyridine Nifedipine (10 μM), a well-known inhibitor of L-type Ca^{2+} channels [37]. The *I–V* curves of peak Ba^{2+} currents showed that regardless of the transfection (EGFP or CRMP-2-EGFP) or treatment (0.3% MPL or 300 μM LCM), the peak current density was similar (Figure 3B). The maximum currents, measured at −20 mV and normalized to cell size, were (in pA/pF; n = 6–8 each): 5.2 ± 0.6 (EGFP control); 5.0 ± 0.7 (EGFP + LCM 300 μM); 5.2 ± 0.8 (CRMP-2-EGFP control); and 5.5 ± 0.6 (CRMP-2-EGFP + LCM 300 μM) (Figure 3C, p >0.05).

We also examined voltage-dependent properties of activation and inactivation of Ba^{2+} currents in these cells. The steady-state activation of Ba^{2+} channels from EGFP and CRMP-2–EGFP over-expressing CAD cells was well described by the Boltzmann relation: $G/G_{max} = 1/\{1+\exp[(V-V_{50})/k_n]\}$, where G is the peak conductance, G_{max} is the fitted maximal G, V_{50} is the half-activation voltage, and k_n is the slope factor. As shown in Figure 4A, for EGFP-expressing neurons, V_{50} was −34.2 ± 0.6 mV (n=8), which was not significantly different from that of CRMP-2–EGFP transfected neurons (−35.1 ± 0.8 mV, n=7; $p > 0.05$, Student's t-test). The slope factors for the Boltzmann fits (mV/e-fold change in conductance) were also similar: 6.2 ± 0.4 mV (n=6) for EGFP transfected neurons and 6.8 ± 0.7 (n=7; p > 0.05, Student's t-test) for CRMP-2–EGFP transfected neurons. Treatment with LCM did not affect V_{50} or *k* parameters in either transfected condition (Figure 4A, B).

The voltage-dependent properties of inactivation were determined by applying 5 second conditioning pre-pulses that ranged successively from −120 mV to +30 mV in 10 mV voltage steps, followed by a 50 ms second step depolarization to 10 mV. The normalized test pulse voltage-peak current amplitude relations was plotted against its corresponding holding potential and fitted with the Boltzmann equation. The voltage dependence of inactivation was similar for currents recorded from EGFP and CRMP-2–EGFP expressing CAD cells, as shown by the conductance versus voltage relations (Figure 4C). For EGFP-expressing CAD cells, V_{50} was −50.8 ± 3.3 mV (n=5) in the absence and −51.9 ± 0.9 mV (n=5) in the presence of LCM, neither value being significantly different from that of CRMP-2–EGFP transfected CAD cells in the absence (−52.6 ± 0.7 mV, n=7) or presence of LCM (−52.7 ± 0.7 mV, n=7); p > 0.05; (Figure 4C, D). The slope factors were also similar: 3.3 ± 0.5 mV (n=5) for EGFP transfected CAD cells; 5.3 ± 0.6 (n=5) for LCM-treated EGFP transfected CAD cells; 4.2 ± 0.5 (n=7) for CRMP-2–EGFP transfected neurons; and 4.2 ± 0.4 (n=7) for LCM-treated CRMP-2–EGFP expressing CAD cells ($p > 0.05$). These results indicate that LCM does not affect the current density or biophysical properties of L-type Ca^{2+} currents.

4. Discussion

As many antiepileptic agents (e.g., carbamazepine, topiramate) exert their functions by interacting with multiple targets, and their efficacy is the sum of beneficial interactions [38], it is important to address any potential actions of newly discovered antiepileptics such as LCM on novel targets. With this rationale, in this study we investigated how LCM affected endogenous neuronal voltage-gated calcium currents as well as channels augmented by overexpression of CRMP-2, a second target of LCM's action. Barium currents via N-type voltage-gated calcium (CaV2.2), a recently identified target CRMP-2 [14], were not affected by LCM even in CRMP-2 overexpressing neurons, establishing that the mechanism of action of lacosamide does not involve these Ca^{2+} channels.

4.1 CRMP-2, Ca^{2+} channels, and transmitter release

In addition to its classically defined roles in neuronal differentiation and axonal outgrowth [10], our laboratory has recently shown that CRMP-2 plays a role in neurotransmitter release via interaction with N-type (and likely P/Q-type) Ca^{2+} channels [14]: (1) CRMP-2 increased

NIH-PA Author Manuscript

NIH-PA Author Manuscript

NIH-PA Author Manuscript

cell surface trafficking of CaV2.2, (2) increased rate and extent of synaptic vesicle recycling, and (3) increased K^+-stimulated glutamate release – all of which were blocked by w-conotoxin, an inhibitor of CaV2.2 [14]. CRMP-2 has been shown to be present at synaptic sites in both developing as well as in adult neurons [14, 39]. Consistent with data inferred from one review [28], we observed that LCM did not affect density, activation or inactivation of native hippocampal Ba^{2+} currents. Neither a short-term nor a long-term treatment with LCM affected Ba^{2+} currents via the presynaptic CaV2.2. Additionally, L-type Ca^{2+} currents were also not affected by LCM treatment. Interestingly, in contrast to the CRMP-2 mediated augmentation of N-type Ca^{2+} current density [22, 29], no change was observed in the peak L-type Ca^{2+} current density following CRMP-2 over-expression. While these findings suggest that CRMP-2 couples selectively to N-, antiepileptic treatments but not L-type, Ca^{2+} channels, it is also possible that these differences are due to the cell type itself. For example, CAD cells may already express saturating amounts of CRMP-2 such that further over-expression of CRMP-2 does not elicit any further regulation of the Ca^{2+} currents. Overall, these results are consistent with our preliminary findings showing that multiple LCM does not affect the direct binding between CRMP-2 and intracellular regions of the Ca^{2+} channel (J.M. and R.K., unpublished observations).

CRMP-2-mediated increase in intracellular Ca^{2+} may directly impact transmitter release. CRMP-2 expression and CRMP-2 mediated neuritogenesis are upregulated upon application of the neurotrophic factor glial cell line-derived neurotrophic factor (GDNF) [40] which has been shown to suppress seizures in animal models of epilepsy [41], suggesting a link between CRMP-2 expression and epilepsy. Interestingly, application of GDNF augments Ca^{2+} currents, presumably via N-type Ca^{2+} channels [42]. While the mechanism underlying GDNF's suppression of seizure activity and augmentation of CaV2.2 activity are presently unclear, an increase in CRMP-2 expression may explain both findings. Although N- and P/Q-type account for a large portion of the Ca^{2+} influx required for triggering fast transmitter release [15], L- and R-type channels have also shown to be involved at a variety of central synapses [43–46]. We found that L-type channels, studied in the model CAD cell line, were not affected by lacosamide treatment. Additional Ca^{2+} imaging with Fura2-AM demonstrated that, in the absence of any calcium channel blockers present, LCM does not affect depolarizatrion-evoked calcium release in neurons (J.M. and R.K., unpublished observations), likely ruling out Ca^{2+} influx via R- or T-type channels.

While our studies did not address the effects of LCM on T-type channels, there is one previous review which suggests that low-voltage activated T-type calcium channels are not affected by acute LCM application [28]. Nevertheless, modulation of T-type calcium channels has been reported for other antiepileptics such as ethosuximide and gabapentin [47–49], which have been primarily effective as antiepileptic treatments for absence seizures. However, because of their unique gating properties (i.e., activation at potentials more positive than −60 mV, peak current achieved at −30 mV, rapid inactivation, slow deactivation, contribution to 'window currents' which can engender membrane bistability), they can support rthymic, high-frequency activity thus making them useful targets in chronic pain [50]. It is under these pain conditions where LCM may become relevant to T-type channel activity. LCM has already been shown to be useful in muscle pain [51], tumor- and chemotherapy-induced cancer pain [52], and animal models of chronic inflammatory pain [53].

4.2 CRMP-2 expression in epilepsy and other pathophysiologies

CRMP proteins have been implicated in both developmental and adult neurological diseases [10]. Protein levels of CRMP-2 are significantly reduced in an animal model of epilepsy [13] and in human patients with mesial temporal lobe epilepsy [12]. Decreased levels of CRMP-2 have also been found in patients with Down's Syndrome, Alzheimer's disease,

NIH-PA Author Manuscript

NIH-PA Author Manuscript

NIH-PA Author Manuscript

psychiatric disorders (schizophrenic, bipolar disorder or major depression disorder) [10], and neuronal ceroid lipofuscinosis – a childhood neurodegenerative disorder [54]. In contrast, increased CRMP-2 levels have been reported in an animal model of chronic mild stress [55], hyperalgesia [56], traumatic brain injury and cerebral ischemia, and in nerve regeneration [57]. The overexpression of CRMP-2 in our hippocampal culture system results in at most a three-fold change in CRMP-2 protein (*not shown*) which is well within the range of changes reported in these pathophysiological conditions. This change in CRMP-2 elicited increases hippocampal axonal length (*not shown*) but does not affect Ca^{2+} channels.

In conclusion, our results support the contention that LCM does not affect N-, P/Q- and L-type calcium channels. This is an important conclusion in light of the findings of more than one target of action of LCM (i.e., Na^{+} channels and CRMP-2), one of which has been linked to regulation of calcium channel activity [22, 29]. Our results, for the first time, shown that despite an up-regulation of Ca^{2+} currents by CRMP-2, LCM does not affect calcium channel activity, ruling out these important channels as potential considerations in polypharmacy of LCM in epilepsy.

Acknowledgments

We thank Drs. Cynthia Hingtgen, Theodore Cummins, and Brian Jarecki for helpful comments on the manuscript. We would like to thank Joel Brittain for biochemistry and calcium imaging experiments.

References

1. Llinas RR. Intrinsic neuronal ectroresponsiveness and its possible role in epileptogenesis. Funct Neurol. 1986; 1:333–337. [PubMed: 2440769]
2. Czapinski P, Blaszczyk B, Czuczwar SJ. Mechanisms of action of antiepileptic drugs. Curr Top Med Chem. 2005; 5:3–14. [PubMed: 15638774]
3. Beyreuther BK, et al. Lacosamide: a review of preclinical properties. CNS Drug Rev. 2007; 13:21–42. [PubMed: 17461888]
4. Beydoun A, D'Souza J, Hebert D, Doty P. Lacosamide: pharmacology, mechanisms of action and pooled efficacy and safety data in partial-onset seizures. Expert Rev Neurother. 2009; 9:33–42. [PubMed: 19102666]
5. Errington AC, Stohr T, Heers C, Lees G. The investigational anticonvulsant lacosamide selectively enhances slow inactivation of voltage-gated sodium channels. Mol Pharmacol. 2008; 73:157–169. [PubMed: 17940193]
6. Sheets PL, Heers C, Stoehr T, Cummins TR. Differential block of sensory neuronal voltage-gated sodium channels by lacosamide [(2R)-2-(acetylamino)-N-benzyl-3-thoxypropanamide], lidocaine, and carbamazepine. J Pharmacol Exp Ther. 2008; 326:89–99. [PubMed: 18378801]
7. Park KD, et al. Lacosamide isothiocyanate-based agents: novel agents to target and identify lacosamide receptors. J Med Chem. 2009; 52:6897–6911. [PubMed: 19795888]
8. Goshima Y, Nakamura F, Strittmatter P, Strittmatter SM. Collapsin-induced growth cone collapse mediated by an intracellular protein related to UNC-33. Nature. 1995; 376:509–514. [PubMed: 7637782]
9. Wang LH, Strittmatter SM. A family of rat CRMP genes is differentially expressed in the nervous system. J Neurosci. 1996; 16:6197–6207. [PubMed: 8815901]
10. Schmidt EF, Strittmatter SM. The CRMP family of proteins and their role in Sema3A signaling. Adv Exp Med Biol. 2007; 600:1–11. [PubMed: 17607942]
11. Cavazos JE, Cross DJ. The role of synaptic reorganization in mesial temporal lobe epilepsy. Epilepsy Behav. 2006; 8:483–493. [PubMed: 16500154]
12. Czech T, et al. Reduction of hippocampal collapsin response mediated protein-2 in patients with mesial temporal lobe epilepsy. Neurochem Res. 2004; 29:2189–2196. [PubMed: 15672539]
13. Ryu MJ, Lee C, Kim J, Shin HS, Yu MH. Proteomic analysis of stargazer mutant mouse neuronal proteins involved in absence seizure. J Neurochem. 2008; 104:1260–1270. [PubMed: 17973978]

NIH-PA Author Manuscript NIH-PA Author Manuscript NIH-PA Author Manuscript

14. Brittain, JM., et al. Neuroscience Meeting Planner 519.4/C73. 2009. Chicago, IL: Society for Neuroscience; 2009. An atypical role for CRMP-2 in neurotransmitter release via interaction with presynaptic Ca^{2+} channels.
15. Catterall WA, Few AP. Calcium channel regulation and presynaptic plasticity. Neuron. 2008; 59:882–901. [PubMed: 18817729]
16. Dodge FA Jr, Rahamimoff R. On the relationship between calcium concentration and the amplitude of the end-plate potential. J Physiol. 1967; 189:90P–92P.
17. Rahamimoff R, Dodge FA Jr. Regulation of transmitter release at the neuromuscular synapse: the cooperative hypothesis. Electroencephalogr Clin Neurophysiol. 1969; 27:219. [PubMed: 4184195]
18. Llinas RR. Calcium in synaptic transmission. Sci Am. 1982; 247:56–65. [PubMed: 6291149]
19. Gargus JJ. Genetic calcium signaling abnormalities in the central nervous system: seizures, migraine, and autism. Ann N Y Acad Sci. 2009; 1151:133–156. [PubMed: 19154521]
20. Jen JC, et al. Primary episodic ataxias: diagnosis, pathogenesis and treatment. Brain. 2007; 130:2484–2493. [PubMed: 17575281]
21. Goslin K, Banker G. Experimental observations on the development of polarity by hippocampal neurons in culture. J Cell Biol. 1989; 108:1507–1516. [PubMed: 2925793]
22. Brittain JM, et al. An atypical role for collapsin response mediator protein 2 (CRMP-2) in neurotransmitter release via interaction with presynaptic voltage-gated Ca^{2+} channels. J Biol Chem. 2009; 284:31375–31390. [PubMed: 19755421]
23. Wang Y, Brittain JM, Wilson SM, Khanna R. Emerging roles of collapsin response mediator proteins (CRMPs) as regulators of voltage-gated calcium channels and synaptic transmission. Communicative & Integrative Biology. 2010; 3:1–4. [PubMed: 20539772]
24. Chen Y, et al. NS21: re-defined and modified supplement B27 for neuronal cultures. J Neurosci Methods. 2008; 171:239–247. [PubMed: 18471889]
25. Wang Y, et al. In silico docking and electrophysiological characterization of lacosamide binding sites on collapsin response mediator protein 2 (CRMP-2) identifies a pocket important in modulating sodium channel slow inactivation. J Biol Chem. 2010; 285:25296–25307. [PubMed: 20538611]
26. Lorenzon NM, Foehring RC. Characterization of pharmacologically identified voltage-gated calcium channel currents in acutely isolated rat neocortical neurons. II. Postnatal development. J Neurophysiol. 1995; 73:1443–1451. [PubMed: 7643159]
27. Lees G, Stohr T, Errington AC. Stereoselective effects of the novel anticonvulsant lacosamide against 4-AP induced epileptiform activity in rat visual cortex in vitro. Neuropharmacology. 2006; 50:98–110. [PubMed: 16225894]
28. Errington AC, Coyne L, Stohr T, Selve N, Lees G. Seeking a mechanism of action for the novel anticonvulsant lacosamide. Neuropharmacology. 2006; 50:1016–1029. [PubMed: 16620882]
29. Chi XX, et al. Regulation of N-type voltage-gated calcium (CaV2.2) channels and transmitter release by collapsin response mediator protein-2 (CRMP-2) in sensory neurons. J Cell Sci. 2009; 23:4351–4362. [PubMed: 19903690]
30. Grimm C, Holter NI, Draguhn A, Bruehl C. Compensatory increase in P/Q-calcium current-mediated synaptic transmission following chronic block of N-type channels. Neurosci Lett. 2008; 442:44–49. [PubMed: 18602451]
31. Takahashi K, Wakamori M, Akaike N. Hippocampal CA1 pyramidal cells of rats have four voltage-dependent calcium conductances. Neurosci Lett. 1989; 104:229–234. [PubMed: 2554221]
32. Takahashi K, Ueno S, Akaike N. Kinetic properties of T-type Ca^{2+} currents in isolated rat hippocampal CA1 pyramidal neurons. J Neurophysiol. 1991; 65:148–155. [PubMed: 1847969]
33. Newcomb R, et al. Selective peptide antagonist of the class E calcium channel from the venom of the tarantula Hysterocrates gigas. Biochemistry. 1998; 37:15353–15362. [PubMed: 9799496]
34. Takahashi K, Akaike N. Nicergoline inhibits T-type Ca^{2+} channels in rat isolated hippocampal CA1 pyramidal neurones. Br J Pharmacol. 1990; 100:705–710. [PubMed: 2169937]
35. Chameau P, Lucas P, Melliti K, Bournaud R, Shimahara T. Development of multiple calcium channel types in cultured mouse hippocampal neurons. Neuroscience. 1999; 90:383–388. [PubMed: 10215143]

NIH-PA Author Manuscript NIH-PA Author Manuscript NIH-PA Author Manuscript

36. Wang H, Oxford GS. Voltage-dependent ion channels in CAD cells: A catecholaminergic neuronal line that exhibits inducible differentiation. J Neurophysiol. 2000; 84:2888–2895. [PubMed: 11110818]
37. Igelmund P, Zhao YQ, Heinemann U. Effects of T-type, L-type, N-type, P-type, and Q-type calcium channel blockers on stimulus-induced pre- and postsynaptic calcium fluxes in rat hippocampal slices. Exp Brain Res. 1996; 109:22–32. [PubMed: 8740205]
38. Errington AC, Stohr T, Lees G. Voltage gated ion channels: targets for anticonvulsant drugs. Curr Top Med Chem. 2005; 5:15–30. [PubMed: 15638775]
39. Byk T, Dobransky T, Cifuentes-Diaz C, Sobel A. Identification and molecular characterization of Unc-33-like phosphoprotein (Ulip), a putative mammalian homolog of the axonal guidance-associated unc-33 gene product. J Neurosci. 1996; 16:688–701. [PubMed: 8551352]
40. Kodama Y, et al. Induction of CRMP-2 by GDNF and analysis of the CRMP-2 promoter region. Biochem Biophys Res Commun. 2004; 320:108–115. [PubMed: 15207709]
41. Kanter-Schlifke I, Georgievska B, Kirik D, Kokaia M. Seizure suppression by GDNF gene therapy in animal models of epilepsy. Mol Ther. 2007; 15:1106–1113. [PubMed: 17387333]
42. Wang CY, et al. $Ca^{(2+)}$ binding protein frequenin mediates GDNF-induced potentiation of $Ca^{(2+)}$ channels and transmitter release. Neuron. 2001; 32:99–112. [PubMed: 11604142]
43. Belhage B, Frandsen A, Schousboe A. Temporal and spatial differences in intracellular Ca^{++} changes elicited by K+ and glutamate in single cultured neocortical neurons. Neurochem Int. 1996; 29:247–253. [PubMed: 8885283]
44. Tokunaga T, et al. Pharmacological dissection of calcium channel subtype-related components of strontium inflow in large mossy fiber boutons of mouse hippocampus. Hippocampus. 2004; 14:570–585. [PubMed: 15301435]
45. Miyazaki K, Ishizuka T, Yawo H. Synapse-to-synapse variation of calcium channel subtype contributions in large mossy fiber terminals of mouse hippocampus. Neuroscience. 2005; 136:1003–1014. [PubMed: 16226383]
46. Jun K, et al. Ablation of P/Q-type $Ca^{(2+)}$ channel currents, altered synaptic transmission, and progressive ataxia in mice lacking the alpha(1A)-subunit. Proc Natl Acad Sci U S A. 1999; 96:15245–15250. [PubMed: 10611370]
47. Rogawski MA. New Evidence Supporting a Role for T-Type $Ca^{(2+)}$ Channels in Absence Epilepsy and in the Action of Ethosuximide. Epilepsy Curr. 2002; 2:57. [PubMed: 15309167]
48. Lacinova L. Pharmacology of recombinant low-voltage activated calcium channels. Curr Drug Targets CNS Neurol Disord. 2004; 3:105–111. [PubMed: 15078185]
49. Macdonald RL, Kelly KM. Antiepileptic drug mechanisms of action. Epilepsia. 1993; 34(Suppl 5):S1–8. S1–S8. [PubMed: 7687957]
50. Zamponi GW, Lory P, Perez-Reyes E. Role of voltage-gated calcium channels in epilepsy. Pflugers Arch. 2010; 460:395–403. [PubMed: 20091047]
51. Beyreuther BK, Geis C, Stohr T, Sommer C. Antihyperalgesic efficacy of lacosamide in a rat model for muscle pain induced by TNF. Neuropharmacology. 2007; 52:1312–1317. [PubMed: 17360008]
52. Beyreuther BK, et al. Antinociceptive efficacy of lacosamide in rat models for tumor- and chemotherapy-induced cancer pain. Eur J Pharmacol. 2007; 565:98–104. [PubMed: 17395176]
53. Stohr T, Krause E, Selve N. Lacosamide displays potent antinociceptive effects in animal models for inflammatory pain. Eur J Pain. 2006; 10:241–249. [PubMed: 15946870]
54. Benedict JW, Getty AL, Wishart TM, Gillingwater TH, Pearce DA. Protein product of CLN6 gene responsible for variant late-onset infantile neuronal ceroid lipofuscinosis interacts with CRMP-2. J Neurosci Res. 2009; 87:2157–2166. [PubMed: 19235893]
55. Bisgaard CF, et al. Proteomic investigation of the ventral rat hippocampus links DRP-2 to escitalopram treatment resistance and SNAP to stress resilience in the chronic mild stress model of depression. J Mol Neurosci. 2007; 32:132–144. [PubMed: 17873297]
56. Fujisawa H, et al. Involvement of post-translational modification of neuronal plasticity-related proteins in hyperalgesia revealed by a proteomic analysis. Proteomics. 2008; 8:1706–1719. [PubMed: 18340631]

NIH-PA Author Manuscript

NIH-PA Author Manuscript

NIH-PA Author Manuscript

57. Zhang F, Wang S, Signore AP, Chen J. Neuroprotective effects of leptin against ischemic injury induced by oxygen-glucose deprivation and transient cerebral ischemia. Stroke. 2007; 38:2329–2336. [PubMed: 17600230]

NIH-PA Author Manuscript

NIH-PA Author Manuscript

NIH-PA Author Manuscript

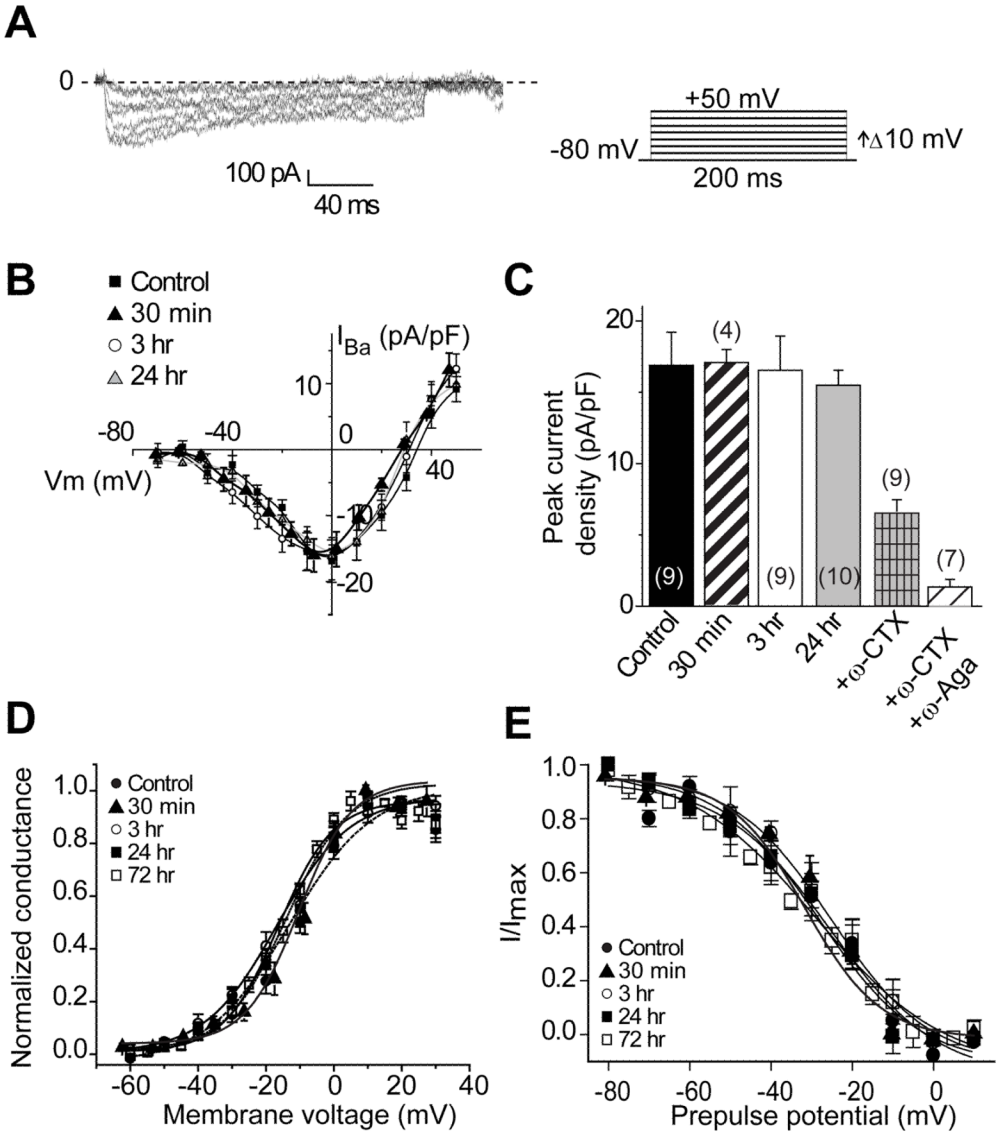

Figure 1.

Voltage-gated Ba^{2+} current density and gating are not affected by acute and chronic treatment with lacosamide. (A) Exemplar current traces obtained from a hippocampal neuron treated with 300 μM LCM for 24 h in response to 200 ms steps in 10 mV increments applied from a holding potential of −80 mV as shown in the voltage protocol on the right. Current traces are shown for every 10 mV step between −70 and +50 mV. Bath solutions contained 1 μM TTX, 10 mM TEA, and 10 μM nifedipine to block Na^+, K^+, and L-type voltage-gated Ca^{2+} channels, respectively. Line labeled 0 indicates the zero-current level. (B) Summary of current-versus-voltage (I–V) relations for neurons treated with MPL (control, *filled squares*), and 300 μM LCM for 30 min (*black filled triangles*), 3 h (*open circles*) or 24 h (*grey triangles*). Peak currents were normalized to cell capacitance. There were no differences in Ba^{2+} current density in any of the conditions at all voltages tested ($p > 0.05$, Student's t-test). (C) Peak current density (pA/pF) measured at 0 mV was similar among the four conditions tested (n=9–10). Omega-conotoxin GVIA (ω-CTX; 1 μM) significantly reduced the current density of control neurons (n=9). A combination of ω-CTX

NIH-PA Author Manuscript

NIH-PA Author Manuscript

NIH-PA Author Manuscript

and the P/Q-blocker ω-Agatoxin (ω-Aga, 500 nM) blocked almost 85–90% of the current. (D) Summary of normalized conductance versus voltage relations for activation of Ba^{2+} current gating in neurons treated with LCM or control (MPL). (E) Summary of normalized current versus voltage relations for inactivation gating of Ca^{2+} currents in neurons treated with LCM or control (MPL). Currents were evoked by 1 sec long voltage steps from −80 mV to +10 mV in 10 mV increments prior to delivering a test pulse to +10 for 200 ms. Values for midpoint of activation and inactivation (V_{50}) and slopes (*k*) are presented in Table 2.

NIH-PA Author Manuscript

NIH-PA Author Manuscript

NIH-PA Author Manuscript

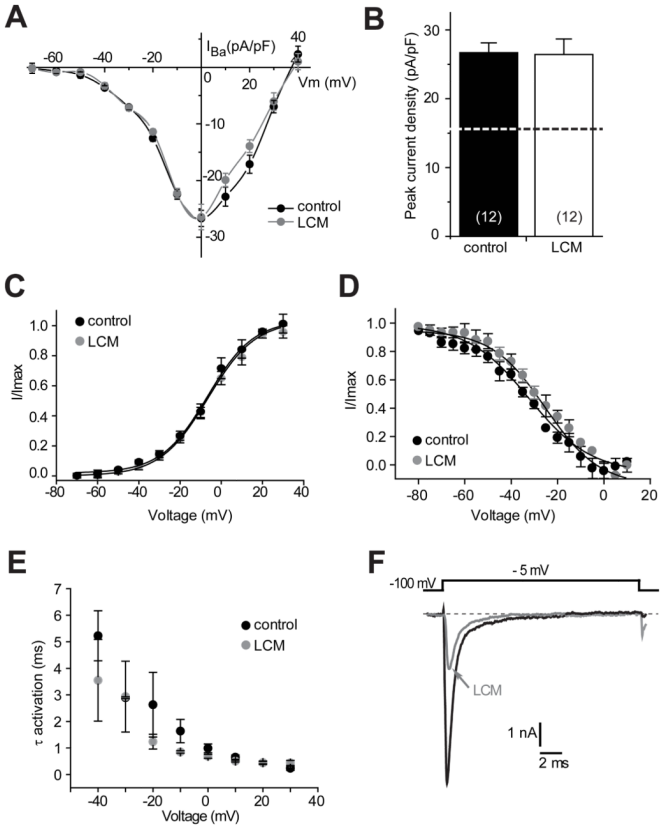

Figure 2.

Voltage-gated Ba^{2+} current density and gating in CRMP-2 overexpressing neurons are not affected by lacosamide. (A) Summary of *I–V* relations for CRMP-2 overexpressing neurons treated with MPL (control, *black circles*) or 300 μM LCM (*gray circles*). Peak currents were normalized to cell capacitance. There were no differences in Ba^{2+} current density between the two conditions at all voltages tested ($p > 0.05$, Student's t-test). (B) Peak current density (pA/pF) measured at 0 mV was similar between CRMP-2 overexpressing neurons treated with 0.01% MPL (*blackbar*) or 300 μM LCM (*white bar*)(n=7 each). As a reference, the peak current density of EGFP-expressing neurons (from Figure 1) is shown as a dotted line. (C) Summary of normalized current versus voltage relations for activation of Ba^{2+} current gating in neurons treated with LCM or control (MPL). (D) Summary of normalized current versus voltage relations for inactivation gating of Ba^{2+} currents in neurons treated with LCM or control (MPL). Neither V_{50} of activation/inactivation nor the slope values derived from the Boltzmann fits of the data revealed any significant differences between the two conditions. (E) Plots of activation time constants were calculated from single exponential fits to the falling phase of the voltage-activated inward Ba^{2+} current. The mean activation time constants for Ca^{2+} currents were not affected by LCM treatment compared with controls ($p > 0.05$, Student's t-test). (F) Representative inward sodium currents from a hippocampal neuron elicited in response to a 20 ms step to −5 mV in the absence (black trace) and presence of 300 μM LCM (gray trace). Robust inhibition of Na^{+} currents was observed.

NIH-PA Author Manuscript

NIH-PA Author Manuscript

NIH-PA Author Manuscript

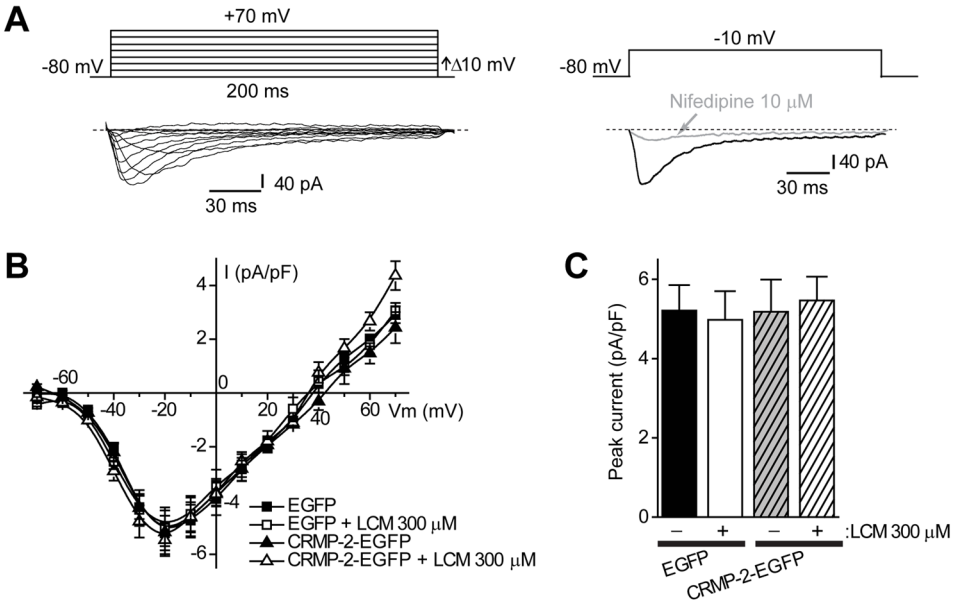

Figure 3.

L-type Ca^{2+} channels are not affected by lacosamide treatment in CAD cells. (A) Voltage protocol used to evoke Ba^{2+} currents (*top*). Representative family of current responses in a CAD cell transfected with CRMP-2-EGFP (*bottom*) elicited by voltage steps from 70 to +70 mV from a holding potential of 80 mV. These inward currents were almost completely eliminated by 10 μM nifedipine (*right*). Current traces were filtered with the Savitzky-Golay smoothing filter for presentation (see Methods for details). (B) Summary of current-voltage (*I–V*) relationships for EGFP and CRMP-2-EGFP-expressing CAD cells in the absence (0.3% MPL) or presence of LCM (300 μM). (C) Peak current density (pA/pF) measured at −10 mV was similar among the four conditions tested (n= 6–8 each). Unless otherwise indicated, values are mean ± S.E.M. and some error bars are smaller than the symbols.

NIH-PA Author Manuscript

NIH-PA Author Manuscript

NIH-PA Author Manuscript

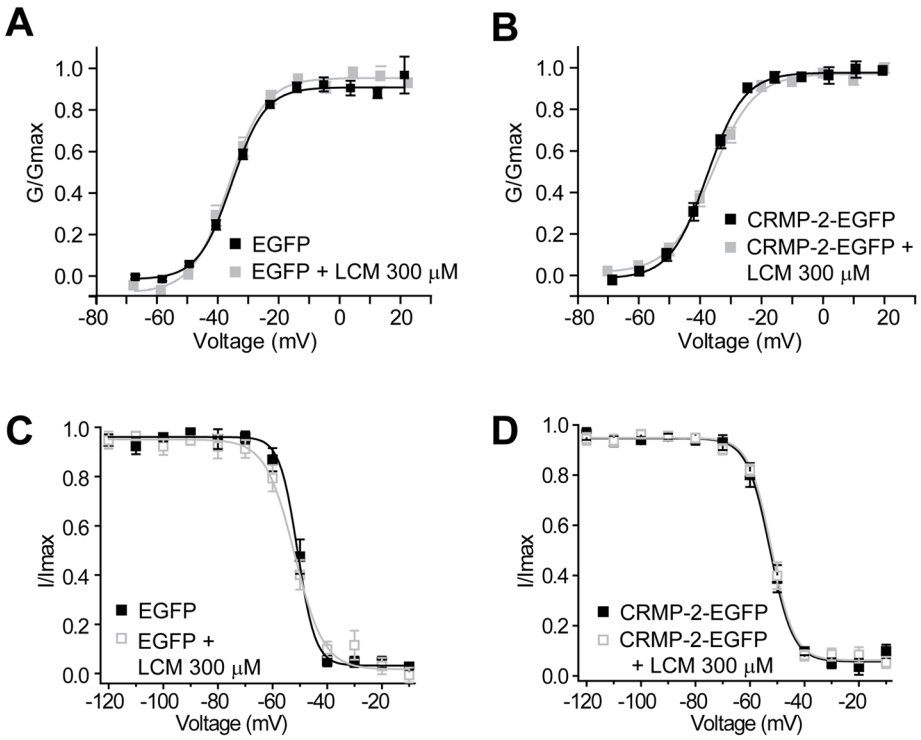

Figure 4.

Activation and inactivation properties of L-type Ca^{2+} channels are not affected by lacosamide treatment in CAD cells. (A, B) Summary of normalized conductance versus voltage relations for activation of L-type Ba^{2+} current gating in EGFP and CRMP-2-EGFP overexpressing CAD cells treated with LCM (300 μM) or control (0.3% MPL). (C, D) Summary of normalized current versus voltage relations for inactivation gating of Ba^{2+} currents in EGFP and CRMP-2-EGFP overexpressing CAD cells treated with LCM or control (MPL). Values for midpoint of activation and inactivation (V_{50}) and slopes (*k*) are presented in the Results section.

NIH-PA Author Manuscript

NIH-PA Author Manuscript

NIH-PA Author Manuscript

Table 1

Composition of recording solutions.

Chemicals (in mM)	Hippocampal neurons				CAD cells	
	Ca^{2+} currents		Na^{+} currents		Ca^{2+} currents	
	External solution[a]	Internal solution	External solution	Internal solution	External solution[b]	Internal solution
4-aminopyridine			4			
ATP Na_2-ATP		2		4		
$BaCl_2$	10				10	
$CaCl_2$			1			0.1
$CdCl_2$			1			
CsCl		110		110		100
d-glucose	10		10		10	
EGTA		10		10		11
GTP		0.2				
HEPES	10	25	10	25	10	10
KCl	5				5	
$MgCl_2$	1		1		1	5
$MgSO_4$		1		5		
NaCl	128		100		125	5
$NiCl_2$			0.1			
TEA-Cl	10		10		10	
Osmolarity (mosM)	*300*	*305*	*310–315*	*290–310*	*300*	*300*
pH	*7.3*	*7.4*	*7.3*	*7.2*	*7.4*	*7.4*

[a]Tetrodotoxin (TTX; 1 μM) and nifedipine (10 μM) were added to the bath to block voltage-gated Na^{+} and L-type Ca^{2+} currents.

[b]TTX (300 nM) was added to the external solution to block Na^{+} currents.

NIH-PA Author Manuscript

NIH-PA Author Manuscript

NIH-PA Author Manuscript

Table 2

Effects of LCM treatment on gating properties of voltage-gated Ca^{2+} channels in hippocampal neurons.

Treatment	Steady-state activation		Steady-state inactivation	
	V_{50}	*k*	V_{50}	*k*
	mV			
Control (0.1–0.3% MPL)	−12.9 ± 2.4 (9)	11.8 ± 1.9 (9)	−26.8 ± 2.0 (9)	12.9 ± 1.9 (9)
LCM 300 μM, 30 min	−13.5 ± 2.9 (4)	11.1 ± 2.5 (4)	−25.8 ± 3.9 (4)	12.2 ± 2.8 (4)
LCM 300 μM, 3 h	−15.2 ± 1.5 (9)	10.1 ± 1.5 (9)	−27.8 ± 1.9 (9)	12.5 ± 1.8 (9)
LCM 300 μM, 24 h	−14.5 ± 2.9 (10)	9.5 ± 2.9 (10)	−26.5 ± 2.4 (10)	12.1 ± 2.8 (10)
LCM 300 μM, 72 h[a]	−16.3 ± 1.1 (7)	8.1 ± 0.9 (7)	−28.8 ± 2.5 (4)	15.8 ± 2.9 (4)

[a]Fresh LCM was added every 24 h.

Numbers in parentheses represent numbers of cells. There were no statistical differences between control and any of the LCM time points for both activation and inactivation gating parameters of midpoint (V_{50}) or slope (*k*)